RESEARCH PAPER

Structural and Optical Characterization of ZnO-Graphene Nanocomposite Quantum Dots

Saba Payrazm[1], Saeid Baghshahi[2,], Zahra Sadeghian[3], Amirtaymour Aliabadizadeh[1]*

* *baghshahi@eng.ikiu.ac.ir*

[1] Department of Materials Engineering, Science and Research Branch, Islamic Azad University, Tehran, Iran
[2] Department of Materials Science and Engineering, Faculty of Engineering, Imam Khomeini International University, Qazvin, Iran
[3] Research Institute of Petroleum Industry (RIPI), Tehran, Iran

Abstract: In this research, zinc oxide quantum dots and graphene nanocomposites were synthesized via two different methods; in the first (direct) method, ZnO-graphene nanocomposites were made by mixing the synthesized zinc oxide and graphene. In the second (indirect) method, zinc nitrate, graphene, and sodium hydroxide were used to make ZnO-graphene nanocomposites. XRD, FTIR, and Raman spectroscopy analyses were used for phase and structural evaluations. The morphology of the nanocomposites was characterized by SEM. The specific surface area and porosity of the samples were characterized by BET analysis. The optical properties of the samples were investigated by photoluminescence and ultraviolet-visible spectroscopy analyses. Results showed that graphene increased the photoluminescence property and shifted the photoluminescence spectrum of the composites towards the visible light spectrum. In the visible light region, the photoluminescence of the synthesized graphene-zinc oxide composite was closer to white light than that of pure zinc oxide. According to the results of BET test, the nanocomposite synthesized by direct method had a higher surface area ($25.7\ m^2.g^{-1}$) and a higher porosity ($0.32\ cm^3.g^{-1}$) than the nanocomposite synthesized by the indirect method with a specific surface area of ($16.5\ m^2.g^{-1}$) and a porosity of ($0.23\ cm^3.g^{-1}$).

Keywords: Quantum dots, Nanocomposite; Graphene, Zinc oxide, Photoluminescence, Photocatalyst.

1. INTRODUCTION

Quantum dots are one of the most practical nanostructures in industry and medicine. In the industry, the quantum dots are used to make LED lights, solar batteries, etc. In medicine, quantum dots are used to design and construct ultra-sensitive nano-bio sensors with higher optical stability than traditional organic pigments. The ratio of surface to volume of samples is increased using quantum dots. Quantum dots have unique properties such as higher optical stability compared to conventional organic pigments with narrower wavelengths of the spectrum that can stimulate the electrons and so on [1-15].

Zinc oxide is a semiconductor. Its straight bandgap at room temperature is 3.36 eV. Zinc oxide is used in thin-film transistors and light-emitting diodes, and the solvothermal method is commonly used for synthesizing zinc oxide quantum dots. [6-16].

Graphene is constructed as the two-dimensional structure of single graphite layers in which carbon atoms are arranged in a hexagonal array. Graphene has the highest electron transfer rate and unique mechanical, optical, thermal, and electro chemical properties [17, 18].

A composite combines two or more materials in which the components are chemically separated and insoluble. Composite refers to a mixture of different materials whose constituents retain their identity, do not dissolve into one another, and do not form a new chemical composition [19, 20].

The addition of carbon-based materials improves the photocatalytic activity of semiconductors. Carbon materials are good electron conductors and can help transfer charge between metal oxides and pollutant molecules. Specifically, graphene, due to its high particular surface area, electronic conductivity, and surface-to-volume ratio, is a significant material [21]. The addition of metal oxides such as ZnO, TiO_2, SnO_2 [22], V_2O_5, Cu_2O [23, 24], Bi_2O_3 [25], and graphene improves the photocatalytic performance. Among them, the graphene-ZnO nanocomposite is more stable. Compared to pure zinc oxide, the luminescence emission intensity of the nanocomposites is drastically reduced. This suggests that the presence of graphene can affect the structure of zinc oxide [26].

Saba Payrazm, Saeid Baghshahi, Zahra Sadeghian, Amirtaymour Aliabadizadeh

In this study, ZnO-graphene nanocomposite quantum dots were synthesized, and their optical properties and microstructure were studied compared to monolithic zinc oxide. The raw materials, graphene and zinc oxide, were synthesized. Graphene oxide was synthesized by the Hammer method [27-29].

The use of graphene and the formation of nanocomposites have improved the photoluminescence properties compared to pure zinc oxide. In other words, with the addition of graphene to zinc oxide and the creation of graphene-zinc nanocomposite, the resulting photoluminescence spectrum ends up containing almost all wavelengths of visible light. This means that the photoluminescence of the synthesized graphene-oxide nanocomposite, in visible light, is closer to white light than that of pure zinc oxide [30].

2. EXPERIMENTAL PROCEDURE

2.1. Synthesis of graphene oxide and graphene

The Hammers method was used to produce graphene oxide. First, 180 ml sulfuric acid (Merck- 112080) with 20 ml phosphoric acid (Merck- 100573) were mixed in a beaker with a magnetic stirrer. Then, 1.5 g graphite powder (Merck- 104206) was added to the mixture of sulfuric acid and phosphoric acid, and the beaker was placed in a water and ice bath to fix the temperature below 10□. Next, 9 g potassium permanganate powder (Merck- 105082) was slowly added to a mixture of acid and graphite, and the suspension was mixed for 15 minutes, and the temperature was increased to 45□ for 24 hours. Then, the mixture was cooled to room temperature. A solution of 3 mL of oxygenated water and 200 mL of deionized water was made, and its temperature was reduced to 0°C. Next, the mixture of acid and graphite is slowly added to a water and oxygenated water solution. Adding the mixture of acid and graphite to the solution of deionized water and oxygenated water caused a strong reaction which changed the color of the mixture to brownish-yellow. Then the suspension was centrifuged for 30 minutes, and the solid was washed with deionized water and hydrochloric acid, with a volume ratio of 1 to 1. In this step, the graphene oxide plates were separated in a deionized water bath under ultrasonic and dried in an oven at 70□ for 12 hours [27, 28].

100 mg of graphene oxide and 100 mL of deionized water were mixed using an ultrasonic mixer for 10 minutes. Then, the solution was transferred to a reflux system and was mixed using a magnetic stirrer at 100□. Then, 1 mL of hydrazine hydrate (Sigma Aldrich- 04604) was added to the solution, and the system was left for 24 hours. After that, the balloon contents were washed with deionized water and ethanol and centrifuged. At the end of this period, brown graphene oxide was restored to black graphene. The graphene was dried at 70□ for 12 hours.

2.2. Synthesis of zinc oxide

For the synthesis of ZnO, 10 mL of a 1 M solution of $ZnSO_4$ (Merck- 108883) was mixed with 10 mL of a solution of 1 M Na_2CO_3 (Merck- 106395) and 1 M NaOH (Merck- 106462) with a volume ratio of 1 to 1 at the temperature of 60□. It made a white suspension.

The suspension was then separated with centrifuging and washed with deionized water. Then, for nucleation and growth of nanoparticles of ZnO, 0.38 g of stearic acid (Merck- 800673) was added to 4.5 mL of a solution of water-ethanol with a volume ratio of 1 to 1, and then 0.5 g ZnO powder was added and mixed. The suspension was transferred to a Teflon container in a stainless-steel autoclave. To complete the reaction, the solution was held at 180□ for 72 hours. The product obtained was separated by centrifuging and washed with ethanol. The powder dried in an oven at 70□ for 12 hours [21, 31].

2.3. Synthesis of graphene-zinc oxide nanocomposite by solvothermal method (Indirect method)

0.2 g graphene was dispersed in a 50 mL solution of ethanol and deionized water with a ratio of 2 to 3 and mixed for 30 min. Zinc nitrate (Merck- 108833) was added to the graphene solution and mixed for 15 minutes to produce a homogeneous dispersion. A diluted sodium hydroxide solution was added to the mixture until a pH value of 12 was obtained and mixed for 30 min. The mixture was transferred to a Teflon stainless steel autoclave and put in an oven at 90□ for 12 hours. The solid precipitation was separated from the solution by centrifugation, repeatedly washed with deionized water and ethanol respectively, and dried at 70□ in an oven for 12 hours [30, 32].

2

2.4. Synthesis of graphene-zinc oxide nano-composite by solvothermal method (Direct method)

0.2 g graphene was re-dispersed in a 50 ml solution of ethanol and deionized water with a ratio of 2 to 3 and was mixed for 30 min. Then, 0.8 g of zinc oxide was added to the solution, and the suspension was mixed at room temperature for 1 hour. The mixture was transferred to a Teflon stainless steel autoclave and put in an oven at 90□ for 10 hours. The solid precipitation was separated from the solution by centrifugation, repeatedly washed with deionized water and ethanol respectively, and dried at 70□ in an oven for 12 hours.

2.5. Characterization of the prepared nano-composites

The diffraction patterns were obtained with an XRD analysis (Philips PW1730) with Cu$-K\alpha$ target with k= 1.54060 Å to identify the final phases. Raman characterization was conducted using a portable Raman device (RIGAKU, Japan) with a 1064 nm wavelength. FTIR analysis was performed using the Vertex 70 Bruker spectrometer with a 4 Cm^{-1} resolution. The morphology of samples was analyzed by SEM instrument (MIRA3, TE-SCAN). Surface area measurements were done by the BET method. First, the samples were heated at 200□ for 1 hour

and then were degassed in a vacuum to remove the contaminants. Then the absorption of nitrogen gas at a constant temperature of 77 K was measured. For analyzing the photocatalytic power of the graphene-zinc oxide nanocomposite, 0.25 g graphene-zinc oxide nanocomposite that was synthesized by the direct method was added to 500 mL solution of 10 ppm methylene blue in deionized water and was exposed by visible white light (NARVA– LT8ET5/760-010 daylight) and was mixed at the same time by a magnetic stirrer. Some samples were taken from the mixture during the light exposure at a specified passing time. 10 mL of methylene blue solution was used in each sample. After taking the samples, they were centrifuged at 5000 rpm for 10 minutes. 5 mL of each taken methylene blue in deionized water samples were subjected to spectrophotometer testing.

3. RESULTS AND DISCUSSION

Figure 1 presents the XRD patterns of graphene, zinc oxide, and graphene-zinc oxide nanocomposites (prepared by direct and indirect methods). According to Figure 1, graphene was synthesized as a single-phase according to the standard card [00-001-0640], zinc oxide was synthesized as a single-phase according to the standard card [01-079-0207].

Fig. 1. Figure 1. The XRD patterns of graphene, zinc oxide, and graphene-zinc oxide nanocomposites prepared by direct and indirect method

*Saba Payrazm, Saeid Baghshahi, Zahra Sadeghian, Amirtaymour Aliabadizadeh*

As shown in Figure 1, graphene-zinc oxide nanocomposites (prepared by direct and indirect methods) have two phases of graphene [00-001-0640] and zinc oxide [01-079-0207], and no new phases were detected.

The FTIR spectra for the graphene-zinc oxide nanocomposites synthesized are shown in figure 2.

According to figures 2a and 2b, for the graphene-ZnO nanocomposites, a characteristic peak at 1501-1638 cm^{-1} corresponding to the stretching vibrations of C=C is observed, which confirms the formation of the graphene structure. FTIR peaks observed at 670, 876, 2852-2922 cm^{-1} for refer to the C-H bonding. The other peak at 1384 cm^{-1} refers to N-O banding, and the peak at 3416 cm^{-1} refers to the O-H group due to moisture absorbed, and the 2034 cm^{-1} peak shows the C≡C banding [33-35].

Figure 3 shows the SEM images of the graphene, zinc oxide, graphene-zinc oxide nanocomposites synthesized by the direct method and graphene-zinc oxide nanocomposites synthesized by the indirect method.
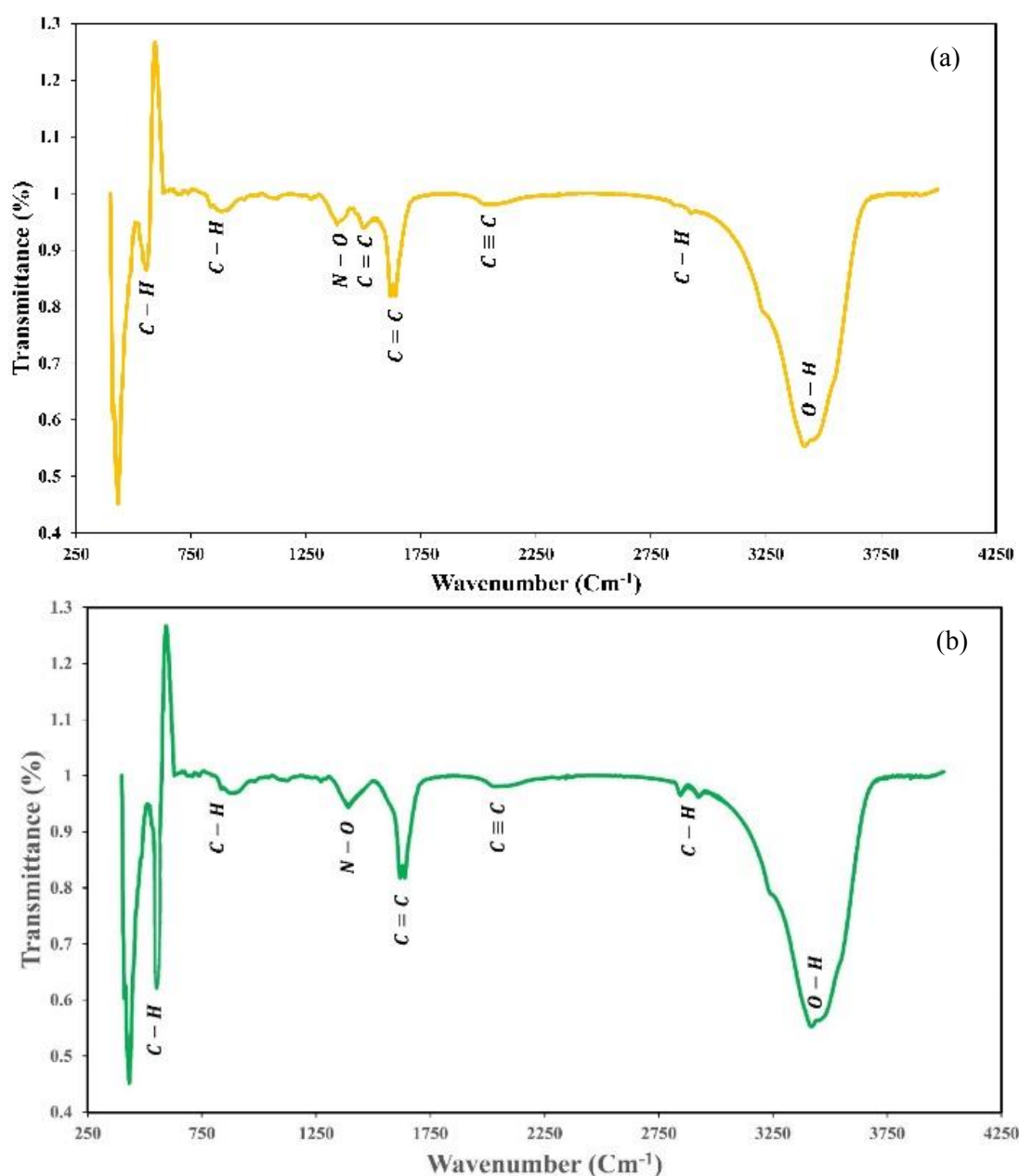
Fig. 2. FTIR spectra of graphene-zinc oxide nanocomposites synthesized by (A) the direct method and (B) indirect method
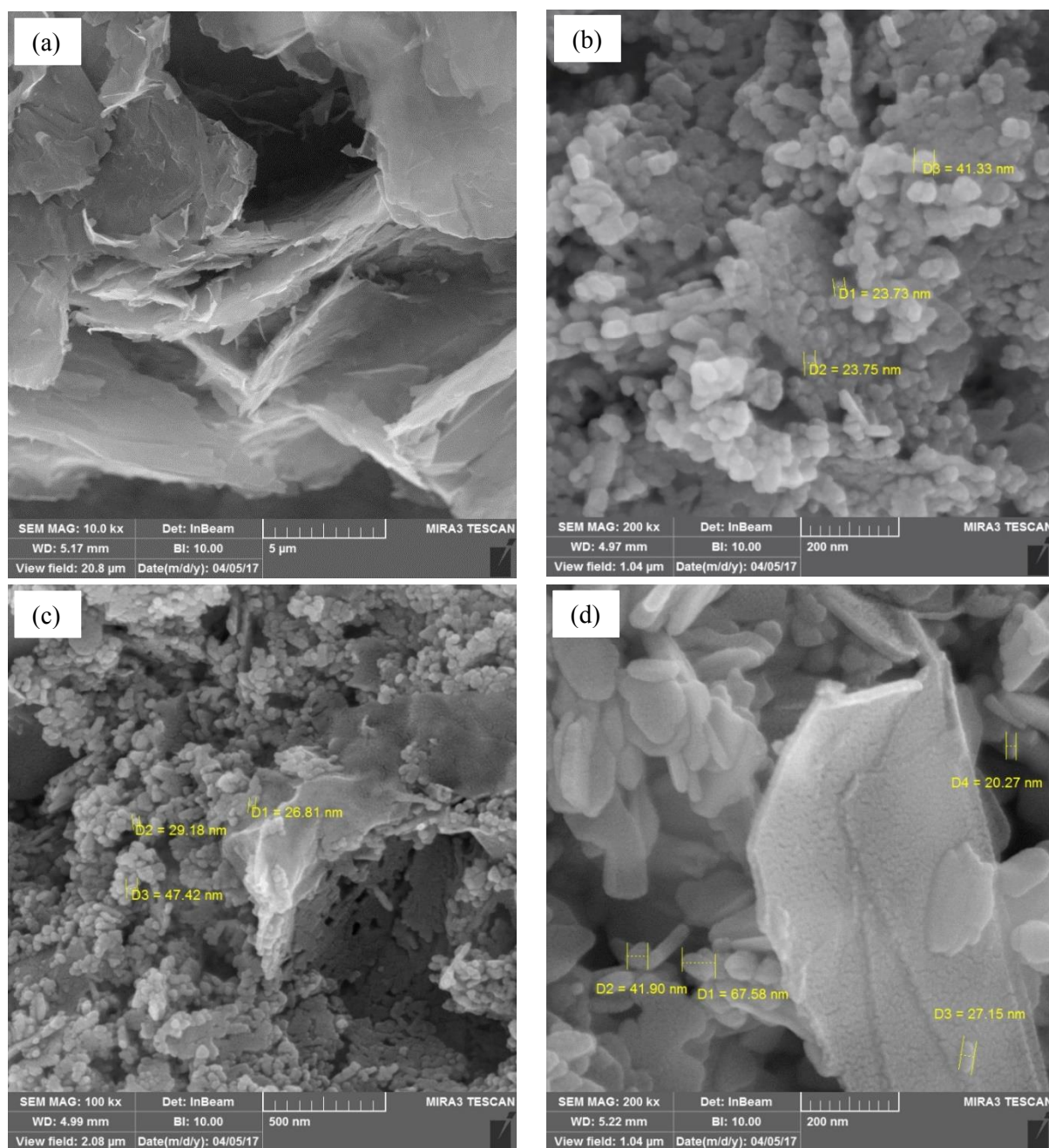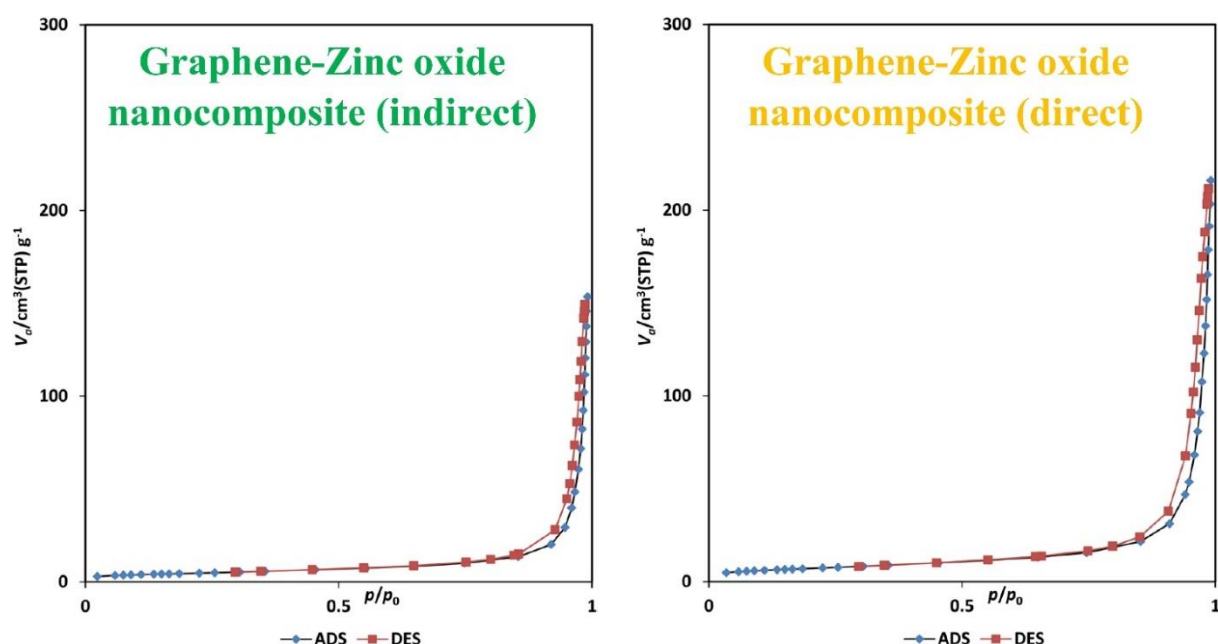
Fig. 3. SEM images of (A) graphene (B) zinc oxide (C) graphene-zinc oxide nanocomposite synthesized by the direct method and (D) graphene-zinc oxide nanocomposite synthesized by the indirect method

According to figure 3, the synthesized graphene has a thickness of about 10 nm, and the synthesized zinc oxide has a spherical morphology with an average diameter of 29 nm. Also, the nanocomposite, which was synthesized by the direct method, has zinc oxide particles with an average diameter of 34 nm. The sample was synthesized by the indirect method has zinc oxide particles with an average diameter of 39 nm.

In the indirect method of synthesizing, zinc oxide particles were formed on the graphene plates in the form of pins and needles, while in the direct method, the particles are spherical. The particle size in the sample synthesized by the direct method is more fine-grained than the one synthesized by the indirect method. Figure 4 shows the BET isotherms of adsorption/desorption of the N_2 gas on the specific surface of both of the graphene-zinc oxide nanocomposites samples that were synthesized by direct and indirect methods.

*Saba Payrazm, Saeid Baghshahi, Zahra Sadeghian, Amirtaymour Aliabadizadeh*

Fig. 4. BET isotherms of adsorption/desorption of the N_2 gas on the specific surface of both of the graphene-zinc oxide nanocomposites samples.

As shown in figure 4 and according to IUPAC classification, these isotherms are type IV. This means the graphene-zinc oxide nanocomposite samples have mesoporous. It can be concluded that the graphene-zinc oxide nanocomposites sample that was synthesized by the direct method has a higher specific surface area. This confirms the results of the SEM images in Figure 4. The size and shape of the porosity of powder particles are also some of the factors affecting photocatalytic properties [30, 36].

Figure 5 shows the BET plot of both graphene-zinc oxide nanocomposites samples synthesized by direct and indirect methods.
According to figure 5, the specific surface area of both graphene-zinc oxide nanocomposites samples synthesized by direct and indirect methods is calculable.
Figure 6 shows the porosity size distribution of both graphene-zinc oxide nanocomposites samples synthesized by direct and indirect methods.
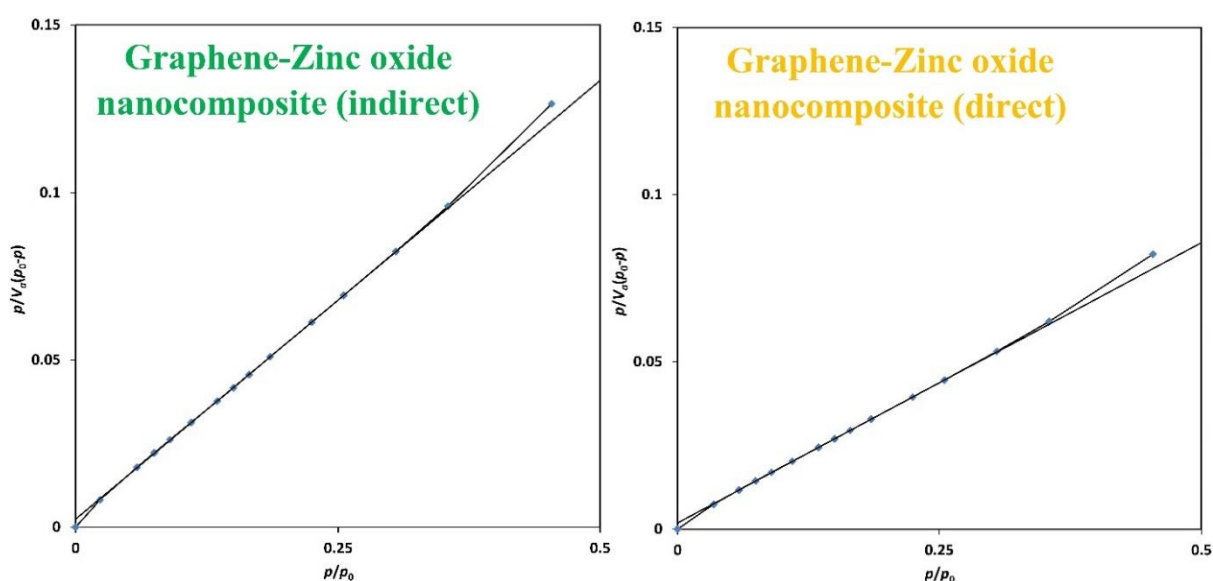
Fig. 5. BET plot of both of the graphene-zinc oxide nanocomposites samples that were synthesized by direct and indirect methods.

6

Fig. 6. The porosity size distribution of both of the graphene-zinc oxide nanocomposites samples that were synthesized by direct and indirect methods.

Figure 6 compares the porosity distribution of the two samples, both of the graphene-zinc oxide nanocomposites samples that were synthesized by direct and indirect methods. According to figure 6, graphene-zinc oxide nanocomposite, which was synthesized by the direct method, has smaller particles.

Table 1 shows the specific surface area, porosity volume, porosity radius, and porosity surface area of both graphene-zinc oxide nanocomposites samples that were synthesized by direct and indirect methods.

Figure 7 shows the results of the photo-luminescence (PL) emission test of graphene, ZnO, and graphene-ZnO nanocomposite samples with an excitation wavelength of 360 nm.

As shown in figure 7, the spectra show a sharp emission peak in the blue region with a maximum of 430 nm, corresponding to the exciton emission of graphene and ZnO. Pure ZnO has higher emission intensity in visible blue spectra due to defect states such as oxygen vacancies in the

structure of ZnO. However, with the formation of the composite, these defects decreased, and the composites have emission in the spectra that are more approached to white light. This might result in an improvement in ZnO applications [30, 36-40].

Due to the Photoluminescence results, the radiation intensity of the graphene-zinc oxide nanocomposite synthesized by the indirect method is more than the direct method. This happened because the particle size in graphene-zinc oxide nanocomposite synthesized by the direct method is smaller than graphene-zinc oxide nanocomposite synthesized by the indirect method, and it causes more internal absorption.

Figure 8 shows the ultraviolet-visible (UV–Vis) absorption spectra of Methylene blue solution samples in response to graphene and ZnO.

Sample in visible light spectra. So, graphene could be used as a composite part with ZnO to increase the photocatalytic power in visible light. Pure ZnO gives a sharp absorption peak at 369 nm corresponding to the bandgap of 3.36 eV.

Table 1. Specific surface area, porosity volume, porosity radius, and porosity surface area of both of the graphene-zinc oxide nanocomposites samples that were synthesized by direct and indirect methods.

Sample	$a_{S, BET}$ (m²/g)	V_P (cm³/g)	$r_{P, Peak\ Area}$ (nm)	a_P (m²/g)
graphene-zinc oxide nanocomposite (direct)	25.684	0.3214	12.17	31.167
graphene-zinc oxide nanocomposite (indirect)	16.455	0.2316	21.86	19.767

Saba Payrazm, Saeid Baghshahi, Zahra Sadeghian, Amirtaymour Aliabadizadeh

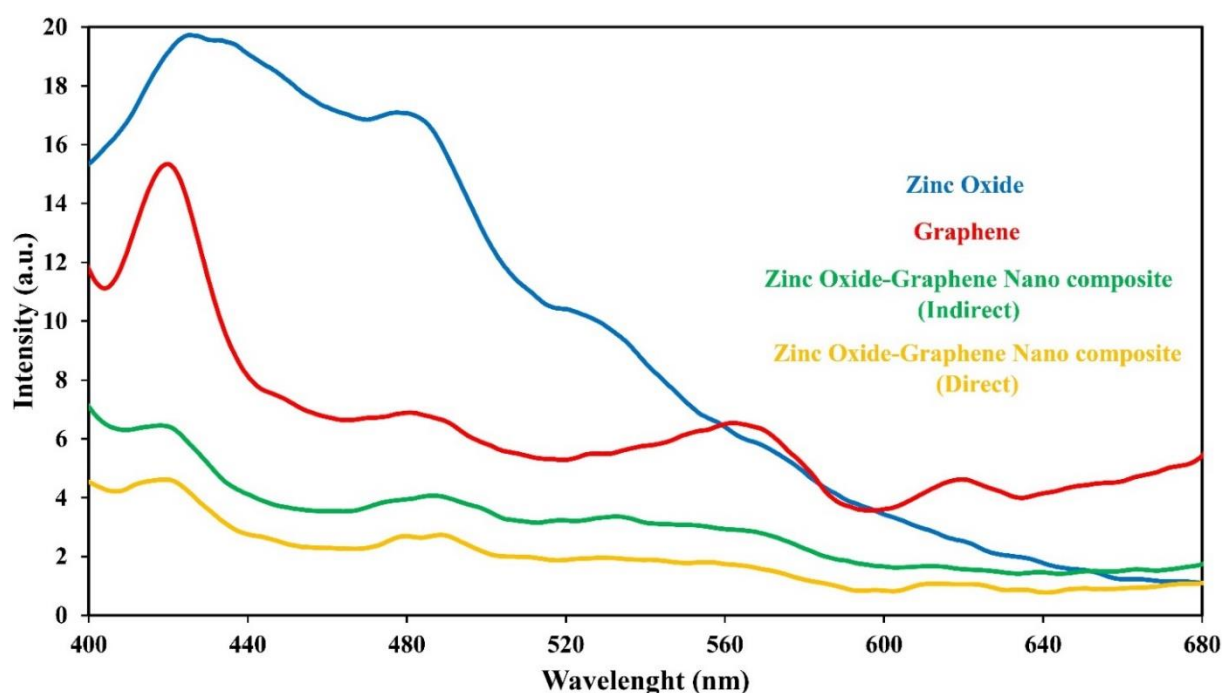**Fig. 7.** Photoluminescence emission spectra for graphene, ZnO, and graphene-ZnO nanocomposites acquired with the excitation wavelength of 360 nm.
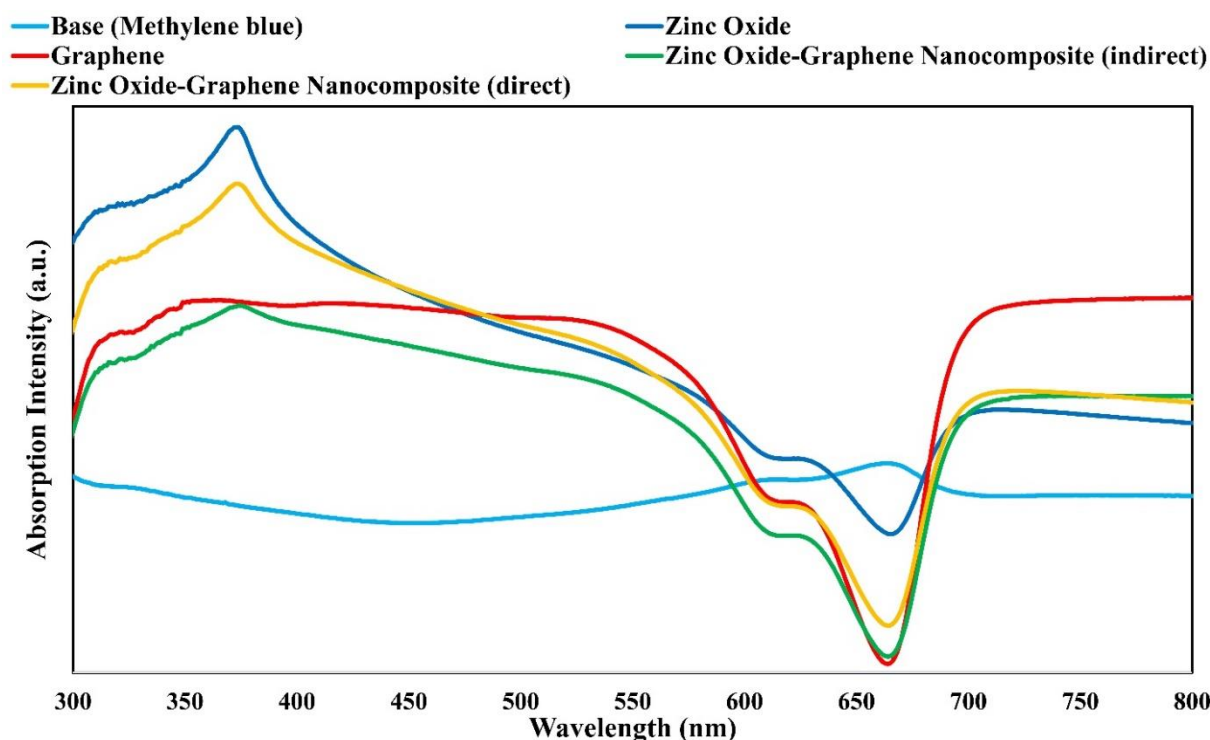

Fig. 8. UV-Visible absorption spectra of Methylene blue solution samples.

As shown in figure 8, the sample containing pure graphene has less absorption than the pure ZnO this indicates a good crystalline ZnO structure that usually shows absorption in the UV region. The position of the 369 nm peak remains unchanged, whereas, only the intensity decreases with the corresponding decrease in ZnO concentration in the nanocomposites. So, variation in the ZnO concentration in the nanocomposites did not cause any changes in the

8

bandgap of the nanocomposites. Also as shown in figure 8, the intensity of the absorption spectrum in graphene-zinc oxide nanocomposite synthesized by the direct method is more than graphene-zinc oxide nanocomposite synthesized by the indirect method. This happened because the particle size in graphene-zinc oxide nanocomposite synthesized by the direct method is smaller than graphene-zinc oxide nanocomposite synthesized by indirect method as shown in Figure 3 (SEM images). It means the effective surface in graphene-zinc oxide nanocomposite synthesized by the direct method is more than graphene-zinc oxide nanocomposite synthesized by the indirect method [27-30].

Figure 9 shows the UV–Vis absorption spectra of Methylene blue solution samples during the exposure time.

According to figure 9, the maximum pick of absorption occurs at 664 nm.

For calculating the concentration of the methylene blue samples, some reference samples were made at specified concentrations and were subjected to UV-Visible absorption spectra testing. For this test, absorption of the light with a wavelength of 664 nm was the maximum pick of Methylene blue light-absorbing, was measured.

The equation of the calculated line is equation 1.

Equation 1:

$$y = Ax + B \tag{1}$$

In this equation, the "A" parameter is 0.1589, and the "B" parameter is 0.0712. According to equation 1, the concentration of the samples was calculated.

The photocatalytic efficiency was calculated by using equation 2.

Equation 2:

$$\text{Efficiency} = \frac{C_0 - C_1}{C_0} \times 100 \tag{2}$$

In this equation, C_0 is the primary, and C_1 is the secondary concentration.

Table 2 shows the efficiency of photocatalytic properties of graphene-zinc oxide nanocomposite that was synthesized by the direct method of decomposing the methylene blue in solution samples during the exposure time. As shown in table 2, 36.41% of methylene blue decomposed at 6 hours of exposure to visible white light.

When samples are exposed to adequate electromagnetic radiation, the electrons absorb energy stimulated and transported to the higher energy levels. These levels are unstable for electrons. So, in the process of returning to the stable situation, the electrons start to react with Methylene blue molecules, which causes decomposing methylene blue.
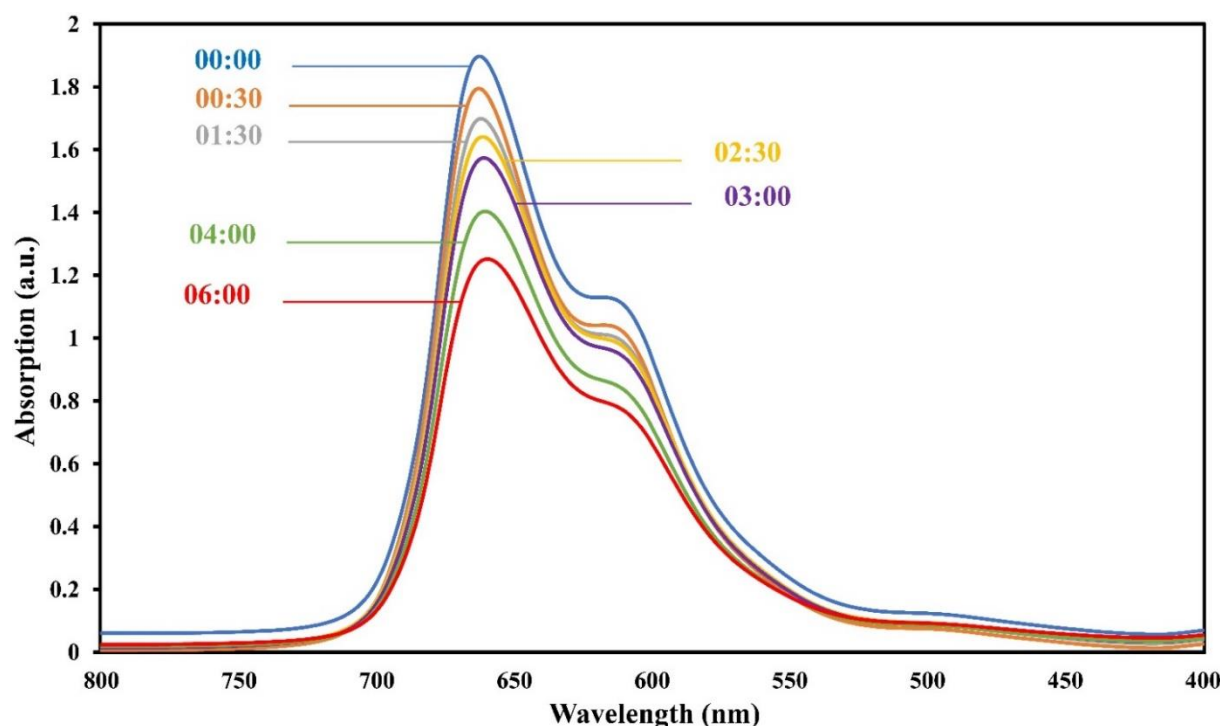

Fig. 9. UV-Visible absorption spectra of Methylene blue solution samples during the exposure time.

Saba Payrazm, Saeid Baghshahi, Zahra Sadeghian, Amirtaymour Aliabadizadeh

Table 2. The efficiency of photocatalytic properties of graphene-zinc oxide nanocomposite that was synthesized by the direct method on decomposing the methylene blue in solution samples during the exposure time.

Sample	1	2	3	4	5	6	7
Exposure time [h]	00:00	00.30	01:30	02:30	03:00	04:00	06:00
Total efficiency (In comparing to the first sample)	-	5.54%	11.07%	14.52%	18.39%	27.82%	36.41%

As a result, due to the changes in methylene blue concentration in the samples, these solutions show different optical absorption rates compared to the reference sample. In other words, the effects of the photocatalytic properties of the samples change the color of Methylene blue solution in the visible wavelength region and change the amount of light absorption of the solution.

Raman spectra for the graphene-ZnO nanocomposites are shown in Fig. 10.

According to figure 10, The "D" and "G" bands at 1284 and 1594 Cm^{-1}, respectively are the characteristic peaks for the carbon components of graphene. The "G" peak arises from the stretching of the C-C bond of Graphite materials and is highly sensitive to strain effects in the sp^2 system. The disordered structure of graphene causes the "D" peak. The "2D" band for graphene is observed at 2705 cm^{-1}, and the "D+G" band is located at 2916 cm^{-1}. The "2D" band is the second-order two-photon process that usually appears due to multilayer-structured graphene. The "2D" band in figure 10 indicates the presence of a few layers of graphene [30, 37, 41-43].

4. CONCLUSIONS

-Graphene-ZnO nanocomposite synthesized by the direct method had particles with an average diameter of 34 nm, while the graphene-ZnO nanocomposite synthesized by the indirect method had particles with an average diameter of 39 nm.

-The specific surface area of graphene-ZnO nanocomposite synthesized by the direct method was larger (25.684 $m^2.g^{-1}$) than that of the one synthesized by the indirect method (16.455 $m^2.g^{-1}$).
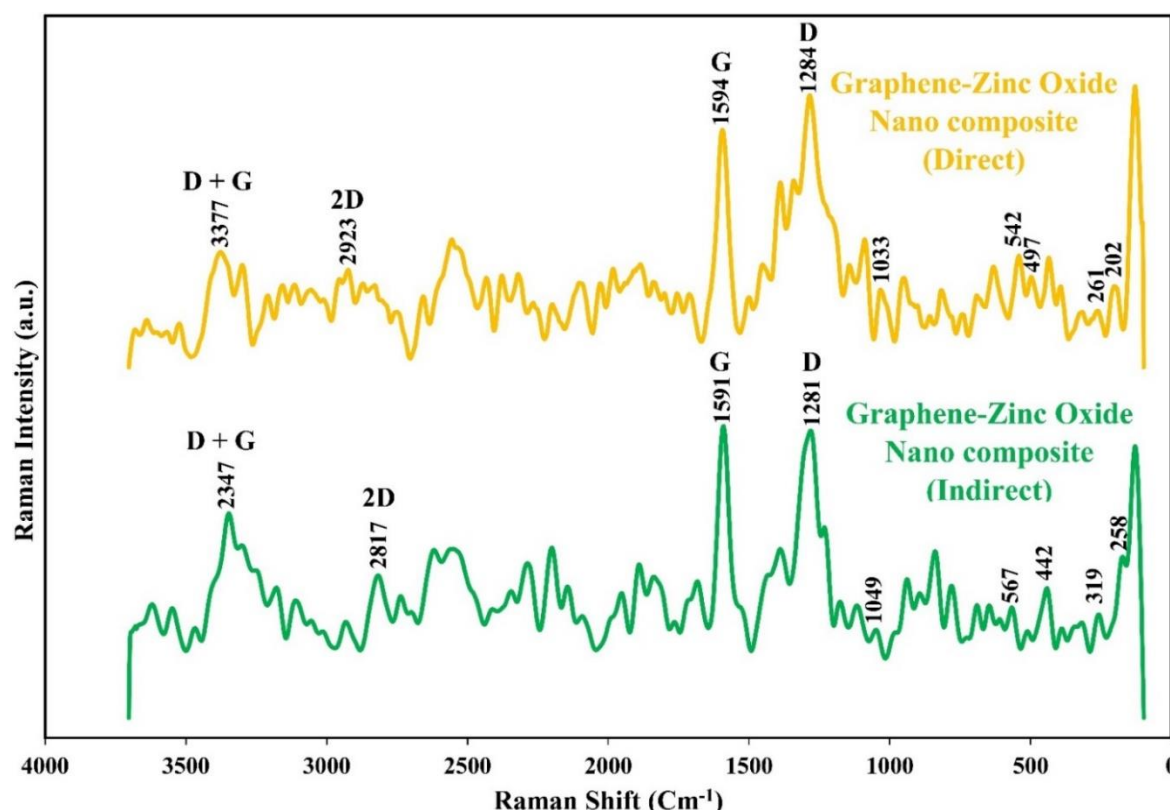
Fig. 10. Raman spectra for graphene, ZnO, and graphene-ZnO nanocomposites were synthesized by direct and indirect methods.

10

-The higher surface area increased the absorption of light and the photocatalytic reaction rate. As a result, the graphene-zinc oxide nanocomposite synthesized by the direct method had higher photocatalytic power than the graphene-zinc oxide nanocomposite synthesized by the indirect method.

-Using graphene in the formation of nanocomposites improved the photo-luminescence property compared to pure zinc oxide. In other words, by adding graphene to zinc oxide, the resulting photoluminescence occurred almost in all of the visible light wavelengths. This means that photoluminescence of the synthesized graphene-zinc oxide nanocomposite, in the visible light spectrum, is closer to the white light than the pure zinc oxide photoluminescence.

REFERENCES

[1] Zhou, W., and Coleman, J.J., "Semiconductor quantum dots", J. Current Opinion in Solid State and Materials Science, 2016, 20, 352-360.

[2] Karakoti, A.S., Shukla, R., Shanker, R. and Singh, S., "Surface functionalization of quantum dots for biological applications", J. Advances in Colloid and Interface Science, 2015, 215, 28-45.

[3] He, X. and Ma, N., "An overview of recent advances in quantum dots for biomedical applications", J. Colloids and Surfaces B: Biointerfaces, 2014, 124, 118-131.

[4] Bonilla, J.C., Bozkurt, F., Ansari, Sh., Sozer, N. and Kokini, J.L., "Applications of quantum dots in food science and biology", J. Trends in food science & technology, 2016, 53, 75-89.

[5] Tayyebi, A., Outokesh, M., Tayebi, M., Shafikhani, A. and Sengor, S.S., "ZnO quantum dots-graphene composites: Formation mechanism and enhanced photocatalytic activity for degradation of methyl orange dye", J. Alloys and Compounds, 2016, 663, 738-749.

[6] Raizada, P., Sudhaik, A. and Singh, P., "Photocatalytic water decontamination using graphene and ZnO coupled photocatalysts: A review", J. Materials Science for Energy Technologies, 2019, 30006-0, 2589-2991.

[7] Liu, Z., Ge, D. and Yang, P., "Structure and interfacial properties investigation for ZnO/graphene interface", J. Materials Chemistry and Physics, 2019, 229, 1-5.

[8] Lonkar, S.P., Pillai, V. and Abdala, A., "Solvent-free synthesis of ZnO-graphene nanocomposite with superior photocatalytic activity", J. Applied Surface Science, 2019, 465, 1107-1113.

[9] Kumar, S., Dhiman, A., Sudhager, P. and V. Krishnan, "ZnO-graphene quantum dots heterojunctions for natural sunlight-driven photocatalytic environmental remediation", J. Applied Surface Science, 2018, 447, 802-815.

[10] Hatamluyi, B. and haghi, Z. Es', "Electrochemical biosensing platform based on molecularly imprinted polymer reinforced by ZnO–graphene capped quantum dots for 6-mercaptopurine detection", J. Electrochimica Acta, 2018, 283, 1170-1177.

[11] Haghshenas, S.S.P., Nemati, A., Simchi, A. and Kim, Ch-Un., "Dispute in photocatalytic and photoluminescence behavior in ZnO/graphene Oxide core-shell nanoparticles", J. Materials Letters, 2019, 240, 117-120.

[12] Salem, M., Akir, S., Massoudi, I., Litaiem, Y., Gaidi, M. and Khirouni, K., "Photoelectrochemical and optical properties tuning of graphene-ZnO nanocomposites", J. Alloys and Compounds, 2018, 767, 982-987.

[13] Rahman, M.U., Xie, F., Li, Y. and Wei, M., "ZnO nanosheets encapsulating graphene quantum dots with enhanced performance for dye-sensitized solar cell", J. Electroanalytical Chemistry, 2019, 30235-8, 1572-6657.

[14] Boukhoubza, I., Khenfouch, M., Achehboune, M., Moses Mothudi, B., Zorkani, I. and Jorio, A., "graphene Oxide/ZnO nanorods/graphene Oxide sandwich structure: The origins and mechanisms of photoluminescence", J. Alloys and Compounds, 2019, 797, 1320-1326.

[15] Ko, K.B., Deul Ryu, B., Han, M., Hong, CH-H., Dinh, D.A. and Vient Guong, T., "Multidimensional graphene and ZnO-based heterostructure for flexible transparent ultraviolet photodetector', J.

Applied Surface Science, 2019, 481, 524-530.

[16] Zhu, L., Liu, Z., Xia, P., Li, H. and Xie, Y., "Synthesis of hierarchical ZnO&graphene composites with enhanced photocatalytic activity", J. Ceramics International, 2018, 44(1), 849-856.

[17] Cai, R., Wu, J-g, Sun, L., Liu, Y-j., Fang, T., Zhu, Sh., Li, Sh.y., Wang, Y., Guo, L-f., Zhao, C-e and Wei, A., "3D graphene/ZnO composite with enhanced photocatalytic activity", J. Materials & Design, 2016, 90, 839-844.

[18] Chen, J., Zhao, M., Li, Y., Fan, S., Ding, L., Liang, J. and Chen, Sh., "Synthesis of reduced graphene Oxide intercalated ZnO quantum dots nanoballs for selective biosensing detection", J. Applied Surface Science, 2016, 376, 133-137.

[19] Soutis, C. and Diamanti, K., "Structural Health Monitoring Techniques for Aircraft Composite Structures", Progress in Aerospace Sciences, 2010, 46, 342 -353.

[20] Daniel, I.M., lshai, O., Engineering Mechanics of Composite Terials, New York, Oxford University Press, 2006, 17-33.

[21] Segovia, M., Sotomayor, C., Gonzaˊlez, G. and Benavente, E., "Zinc Oxide Nanostructures by Solvothermal Synthesis", J. Taylor & Francis, 2012, 555, 40-50.

[22] Cui, H., Liu, Y., Ren, W., Wang, M., Zhao, Y., "Large scale synthesis of highly crystallized SnO_2 quantum dots at room temperature and their high electrochemical performance", J. Nanotechnology, 2013, 24, 345602.

[23] Cheng, L., Wang, Y., Huang, D., Nguyen, T., Jiang, Y., Yu, H., Ding, N., Ding, G. and Jiao, Zh., "synthesis of size-tunable CuO/graphene composites and their high photocatalytic performance", J. Materials Research Bulletin, 2015, 61, 409-414.

[24] Ming Yan, W., Jun Rao, H., Zhi Wei, T., Wei Hua, L. and Jun, Ch., "Reduced graphene oxide–cuprous oxide composite via facial deposition for photocatalytic dye-degradation", J. Alloys and Compounds, 2013, 568, 26-35

[25] Liu, X., Pan, L., Lv, T., Sun, Zh. and Sun, Ch.Q., "Visible light photocatalytic degradation of dyes by bismuth oxide-reduced graphene oxide composites prepared via microwave-assisted method," J. Colloid and Interface Science, 2013, 408,145-150.

[26] Prabhu, S., Megala, S., Harish, S., Navaneethan, M., Maadeswaran, P., Sohila, S. and Ramesh, R., "Enhanced photocatalytic activities of ZnO dumbbell/reduced graphene oxide nanocomposites for degradation of organic pollutants via efficient charge separation pathway", J. Applied Surface Science, 2019, 487, 1279-1288.

[27] Chen, J., Yao, B., Li, Ch. and Shi, G., "An improved Hummers method for eco-friendly synthesis of graphene Oxide", J. Carbon, 2013, 64, 225-229.

[28] Alam, S.N., Sharma, N. and Kumar, L., "Synthesis of graphene Oxide (GO) by modified hummers method and its thermal reduction to obtain reduced graphene Oxide (rGO)", J. Graphene, 2017, 6, 1-18.

[29] Bai, X., Sun, Ch., Liu, Di., Luo, X., Li, Di., Wang, J., Wang, N., Chang, X., Zong, R. and Zhu, Y., "Photocatalytic degradation of deoxynivalenol using graphene/ZnO hybrids in aqueous suspension", J. Applied Catalysis B: Environmental, 2017, 204, 11-20.

[30] Beura, R. and Thangadurai, P., "Structural, optical and photocatalytic properties of graphene-ZnO nanocomposites for varied compositions", J. Physics and Chemistry of Solids, 2017, 102, 168-177.

[31] Siva Kumar, S., Venkateswarlu, P., Rang Rao, V. and Nageswara Rao, G., "Synthesis, characterization and optical properties of zinc oxide nanoparticles," J. International Nano Letters, 2013, 3:30.

[32] Raphael Ezeigwe, E., Tan, M. TTT, Sim Khiew, P. and Wee Siong, Ch., "One-step Green synthesis of graphene/ZnO nanocomposites for electrochemical capacitors", J. Ceramics International, 2015, 41, 715-724.

[33] Zamiri, G. and Bagheri, S., "Fabrication of green dye-sensitized solar cell based on ZnO nanoparticles as a photoanode and graphene quantum dots as a photo-sensitizer", J. Colloid and Interface Science, 2018,511, 318-324.

[34] Sun, L., Zhou, X., Zhang, Y. and Guo, T., "Enhanced field emission of graphene-ZnO quantum dots hybrid structure", J. Alloys and Compounds, 2015, 632, 604-608.

[35] Sandhya, P.K., Jose, J., Sreekala, M.S., Padmanabhan, M., Kalarikkal, N. and Thomas, S., "Reduced graphene oxide and ZnO decorated graphene for biomedical applications", J. Ceramics International, 2018, 44, 15092-15098.

[36] Rahimi, K., Yazdani, A. and Ahmadirad, M., "Graphene quantum dots enhance UV photoresponsivity and surface-related sensing speed of zinc oxide nanorod thin films", J. Materials and Design, 2018, 140, 222-230.

[37] Kumar Mandal, S., Dutta, K., Pal, S., Mandal, S., Naskar, A., Kumar Pal, P., Bhattacharya, T.S., Singha, A., Saikh, R., De, S. and Jana, D., "Engineering of ZnO/rGO nanocomposite photocatalyst towards rapid degradation of toxic dyes", J. Materials Chemistry and Physics, 2019, 223, 456-465.

[38] Lu, T., Pan, L., Li, H., Zhu, G., Lv, T., Liu, X., Sun, Zh., Chen, T. and Chua, D. HCC, "Microwave-assisted synthesis of graphene–ZnO nanocomposite for electrochemical supercapacitors", J. Alloys and Compounds, 2011, 509, 5488-5492.

[39] Kavitha, T., Gopalan, A.I., Lee, K-P and Park, S-Y, "photocatalytic and antibacterial properties of graphene–ZnO nanoparticle hybrids", J. Carbon, 2012, 50, 2994-3000.

[40] Xue, B. and Zou, Y., "Photocatalytic Activity of ZnO–Graphene Composite", J. Colloid and Interface Science, 2018, 529, 306-313.

[41] Aziz, TNTA, Rosli, A.B., Yusoff, M.M., Herman, S.H. and Zulkifli, Z., "Transparent hybrid ZnO-graphene film for high stability switching behavior of memristor device", J. Materials Science in Semiconductor Processing, 2019, 89, 68-76.

[42] Iatsunskyi, I., Baitimirova, M., Coy, E., Yate, L., Viter, R., Ramanavicius, A., Jurga, S., Bechelany, M. and Erts, D., "Influence of ZnO/graphene nanolaminate periodicity on their structural and mechanical properties", J. Materials Science & Technology, 2018, 34, 1487-1493.

[43] Jiao, Zh., Guan, X., Wang, M., Wang, Q., Xu, B., Bi, Y. and Song Zhao, X., "Undamaged depositing large-area ZnO quantum dots/RGO films on photoelectrodes for the construction of pure Z-scheme", J. Chemical Engineering, 2019, 356, 781-790.